Innovation Brief

Shrink-Induced Single-Cell Plastic Microwell Array

Michelle Khine, Ph.D.
University of California
Irvine, CA

*Valerie Lew, Diep Nguyen, and Michelle Khine**
Department of Biomedical Engineering, University of California, Irvine, CA

Keywords:
single-cells,
micro-arrays,
stem cells

The ability to interrogate and track single cells over time in a high-throughput format would provide critical information for fundamental biological understanding of processes and for various applications, including drug screening and toxicology. We have developed an ultrarapid and simple method to create single-cell wells of controllable diameter and depth with commodity shrink-wrap film and tape. Using a programmable CO_2 laser, we cut hole arrays into the tape. The tape then serves as a shadow mask to selectively etch wells into commodity shrink-wrap film by O_2 plasma. When the shrink-wrap film retracts upon briefly heating, high-aspect plastic microwell arrays with diameters down to 20 μm are readily achieved. We calibrated the loading procedure with fluorescent microbeads. Finally, we demonstrate the utility of the wells by loading fluorescently labeled single human embryonic stem cells into the wells. (JALA 2011;■:■–■)

Introduction

Quantitative data from a large number of individual cells provide a wealth of information and insight typically obscured by bulk measurements. Bulk population experiments output the mean value of a parameter of interest, whereas single-cell experiments allow for investigating the distribution of that parameter.[1,2] This is an important distinction that even cells that are identical genetically exhibit marked variations in gene expression.[3] Information on a cell's time- or stimulus-dependent gene expression is lost when the sample's specific signal is diluted with those of surrounding cells, which do not exhibit the same expression. Heterogeneity in behavior across single cells, observable even when the populations' behavior is reproducible and predictable, suggests that it cannot be deterministically described.[4]

Although commercially available techniques currently exist to acquire single-cell data in a high-throughput fashion, such as flow cytometry, dynamic information is unattainable because the same cell cannot be tracked over time. Moreover, with flow cytometry, the output is either a single absorbance or fluorescence profile per cell. Although automated microscopy enables longitudinal studies, imaging is typically nontrivial; cells in suspension require a method of immobilization, whereas confluent cells have an inherently nonuniform shape and confluency-dependent distribution that makes image analysis complex.

Microsystems, with their fine spatial and temporal resolution and control, are ideally suited for—and in many cases, enable—such small-scale interrogations and have demonstrated their utility in cell culture,[5,6] studying cell behavior and response,[7,8] cell sorting,[9,10] cell lysis,[11,12] sample preparation,[13,14] and stem cell studies.[15,16] Such arrays hold great potential for high-throughput drug screening and toxicology studies. There have been several recent comprehensive reviews on technologies for single-cell analyses.[2,17,18]

However, to truly realize the full potential and utility of microsystems to address important biological questions, these microtools need to be accessible

*Correspondence: Michelle Khine, Ph.D., Department of Biomedical Engineering, University of California, 3113 Natural Sciences II, Irvine, CA 92697; Phone: +1.949.824.4051; E-mail: mkhine@uci.edu

2211-0682/$36.00

doi:10.1016/j.jala.2011.06.003

to—and influenced by—experimental biologists and chemists. To move from proof of concept to functional tools, single-cell analysis microsystems need to be designed specifically for quantitative hypothesis-driven biological experiments and compatible with laboratory automation.

Although there have been many recent demonstrations of such systems, patterning such fine features for single cells studies typically necessitates processes such as standard photolithography to make the wells directly in silicon or make molds for polydimethylsiloxane (PDMS), polyethylene glycol, agarose, or plastic wells.[1,8,16,19] Such techniques require expensive capital equipment and expertise typically not available in biological laboratories. As such, there have been several recent demonstrations of innovative solutions circumventing the need for traditional photolithography to make single-cell microwells. For example, Liu et al.[20] developed a PDMS microwell array by molding close-packed 10- or 20-μm polystyrene beads that were melted on glass. Although this resulted in a high density of close-packed wells, the depth of the wells was limited to less than 10 μm. Moreover, this manual approach makes automation and scalability difficult. Instead of polystyrene beads, Park et al.[21] molded microwells by "ice lithography"; by leveraging surface tension of liquid droplets and their subsequent phase transition to ice, they were able to produce concave wells. However, such an approach yields a heterogeneous size population of microwells.

We have developed an ultrarapid and simple method to create single-cell wells of controllable diameter and depth with commodity shrink-wrap film and tape. Using a programmable CO_2 laser, we cut holes into the tape. This tape with a hole array will function as a shadow mask to selectively etch wells into the commodity shrink-wrap film with an O_2 plasma etcher. This allows us to create microwell arrays with diameters down to 20 μm and depths to almost 40 μm (Fig. 1). Because of the ability to achieve high-aspect ratios and unique mushroom-shaped wells, the cells or beads can be rigorously rinsed after loading without washing out the contents of the wells. Therefore, media or drug compounds can also be easily exchanged. Furthermore, these microwells have an increased surface area as seen in the roughened surfaces detailed in the scanning electron micrographs (SEM), which are not easily achieved in standard fabrication processes (Fig. 2).

As a calibration, we successfully captured single polystyrene beads in up to 70% of the wells. Notably, these chips are made of polyolefin (PO), and therefore, this approach enables us to move away from PDMS yet still achieve rapid prototyping. Recent studies have highlighted the inherent drawbacks of PDMS.[22] Therefore, translating to hard plastics commonly used for microtiter plates is attractive but typically difficult to achieve. Interestingly, because of the roughened surface and increased surface area caused by the plasma etching and subsequent shrinkage, this could be leveraged for enhanced protein adsorption (Figs. 2 and 3).[23] With proteins attached to the three-dimensional surface of the wells, studying cell adhesion in the wells may also be possible.[24] Finally, we loaded cells into the wells; the stochastic loading of cells also allows the parallel examination of cell-to-cell studies.

Methods and Materials

Fabrication of the Microwells

To create masks, a CO_2 laser (VersaLaser VLS-2.30, Universal Laser Systems Inc., Scottsdale, AZ) was used to make patterned cut through holes in the sealing tape (Nunc sealing tape, Thermo Fisher Scientific, Rochester, NY) (Fig. 1A). The hole array design was created using a CAD software (AutoCAD, Autodesk, San Rafael, CA). All well sizes were

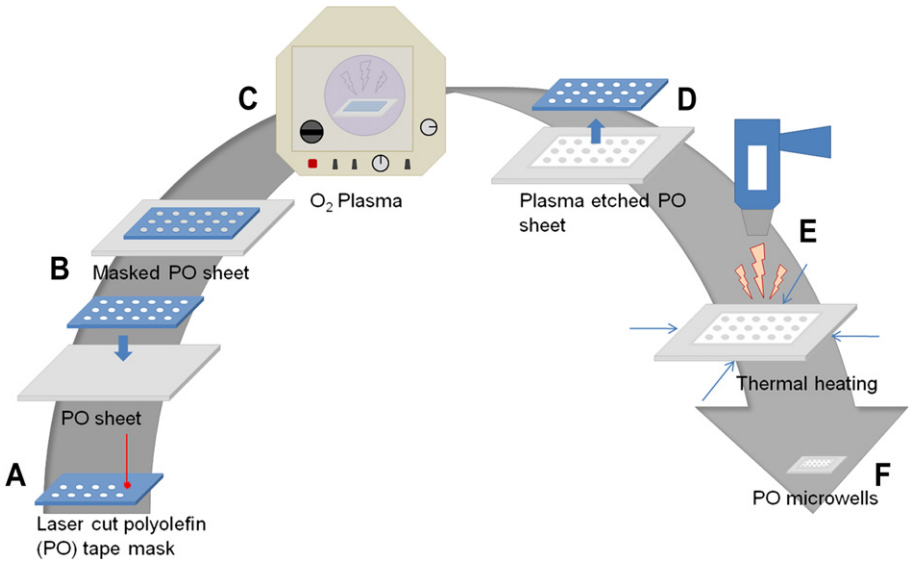

Figure 1. Fabrication process diagram. (A) Laser cutting of PO tape to create a mask, (B) adhering the mask to a PO sheet, (C) plasma etching the substrate, (D) removal of the mask from the PO sheet, and (E) shrinking of the plasma-etched PO sheet using a heat gun to achieve microwells (F).

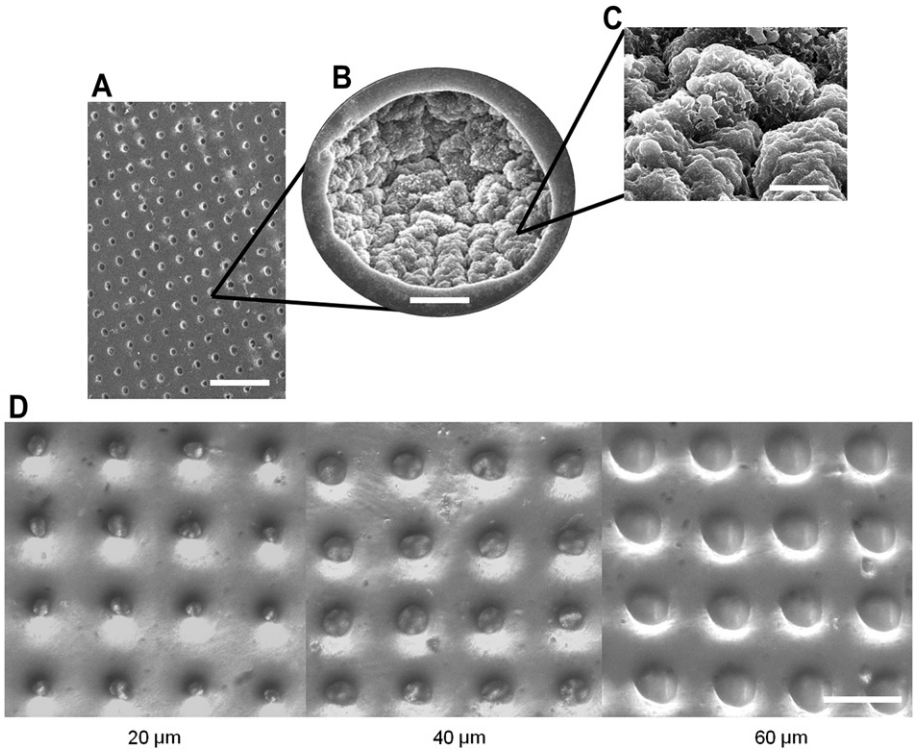

Figure 2. Characterization of microwells. (A) SEM of microwell array. Scale bar is 100 μm. (B) SEM of single well. Scale bar is 10 μm. (C) SEM of well microstructures. Scale bar is 3 μm. (D) Microwells of 20-, 40-, and 60-μm diameter. Scale bar is 100 μm.

made from the same CAD design with a pattern hole size of 0.03 mm; different sizes were achieved by varying the speed and power settings. To make mask holes of approximately 120 μm (to achieve final well sizes of 20 μm), a power setting of 7 and speed of 10 were used. For mask holes of approximately 180 μm (to achieve final well sizes of 40 μm), a power setting of 10 and a speed of 8 were used. Finally, for mask holes of approximately 250 μm (to achieve final well sizes of 60 μm), a power setting of 15 and a speed of 7 were used.

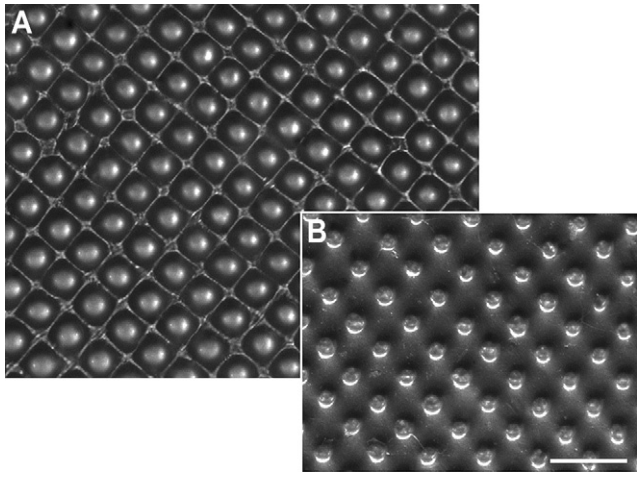

Figure 3. (A) Top surface of microwells. (B) Bottom surface of microwells. Scale bar is 200 μm.

PO shrink film (Multilayer shrink film 955D, Sealed Air Nexcel Corporation, Elmwood Park, NJ) with a thickness of 1 mil (0.0245 mm) adhered to a polyester backing of 3 mil (0.0735 mm) thickness was used to fabricate the 40- and 60-μm sized wells. Thinner shrink film without a backing (Cryovac D-film LD935, Sealed Air Corporation, Elmwood Park, NJ) with a thickness of 0.45 mil (0.0110 mm) was used to fabricate the 20-μm sized wells. PO sheets were cut into 1×2.5 in. pieces and taped lengthwise onto glass slides. The laser cut masks were then adhered on to the top of the PO pieces and treated with O_2 plasma (Plasma Prep II; SPI Supplies, West Chester, PA) for 5, 15, 25, or 35 min (Fig. 1B,C).

After plasma treatment, the adhesive masks were removed, and the plasma etched PO pieces were thermally shrunk at 400 °C for 1−2 min with a heat gun (HL 1810S, Steinel, Bloomington, MN) (Fig. 1D,E). The shrunken PO pieces were then trimmed and mounted onto a 48-well plate with PDMS.

Characterization of Microwells

The microwells were characterized by SEM (S-4700-2 FE-SEM, Hitachi, Schuamburg, IL). Samples were sputter coated with 3 nm of gold or palladium (Polaron SC7620, Quorum Technologies LTD, Ashford, Kent, UK) and then imaged at 30, 1.5K, and 10K magnifications using a 10-kV electron beam (Fig. 2). To determine the diameters of the wells, pictures were taken using an inverted microscope

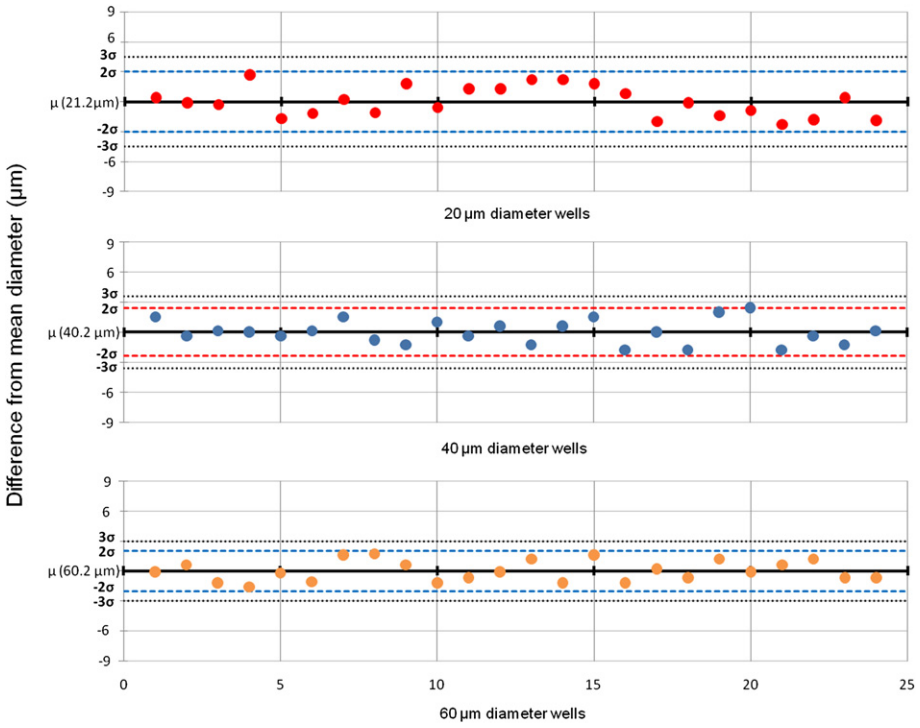

Figure 4. Diameter characterization for 20-, 40-, and 60-µm wells. Diameters range from 18.9 to 23.9 µm, 38.4 to 42.6 µm, and 58.6 to 61.9 µm for 20-, 40-, and 60-µm wells, respectively.

(Olympus IX51, Center Valley, PA) with an attached camera (QICAM 12-bit Mono Fast 1394, Surrey, BC, CAN). The full width/half maximum from the intensity profile of the grayscale images were used to define the diameter of the wells (Fig. 4). Optical characterization of the polymer was performed and previously reported by Taylor et al.[25] Briefly, the preshrunk PO thin film exhibits a relatively minimal autofluorescence and a broad optical transmission in its preshrunk state; these properties, however, diminished on shrinkage as a function of rate and duration of cooling after shrinkage. Thus, it may be possible to minimize the level of opacity by controlling the cooling rate after shrinkage. As it is, we were able to image through the plastic with a standard inverted microscope.

To determine the heights of the wells, the wells were molded into PDMS and then cross sections were taken. The cross-sectional plane with the maximum height correlated with the midplane, and the height was measured using the aforementioned microscope and camera setup. Height measurements were then taken similarly to the diameter measurements for the various plasma times of 5, 15, 25, and 35 min (Fig. 5A). Cross-sectional pictures of the PDMS mold were inverted to better clearly represent the well heights (Fig. 5B).

Bead and Cell Loading

To load beads, the microwell devices, which each contain approximately 1.04×10^3 wells, were bonded to the bottom

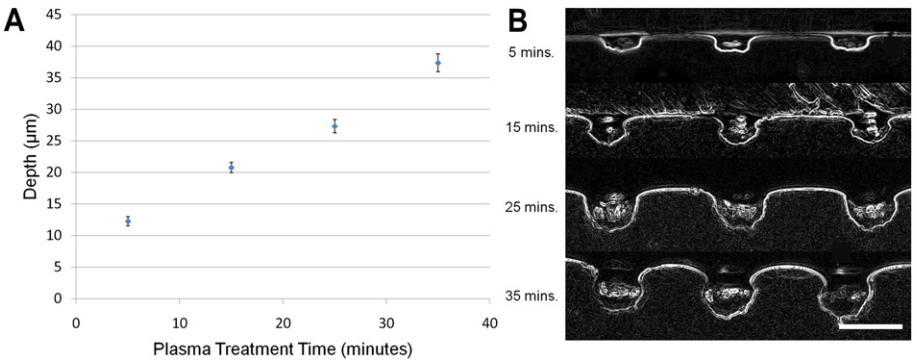

Figure 5. Effect of plasma treatment time on well depth. (A) Plot of microwell depth versus plasma treatment time for 20-µm wells. (B) Cross sections of PDMS molds of microwells using plasma treatment times of 5, 15, 25, and 35 min. Longer treatment times generate deeper wells. Scale bar is 50 µm. *Note:* image inverted.

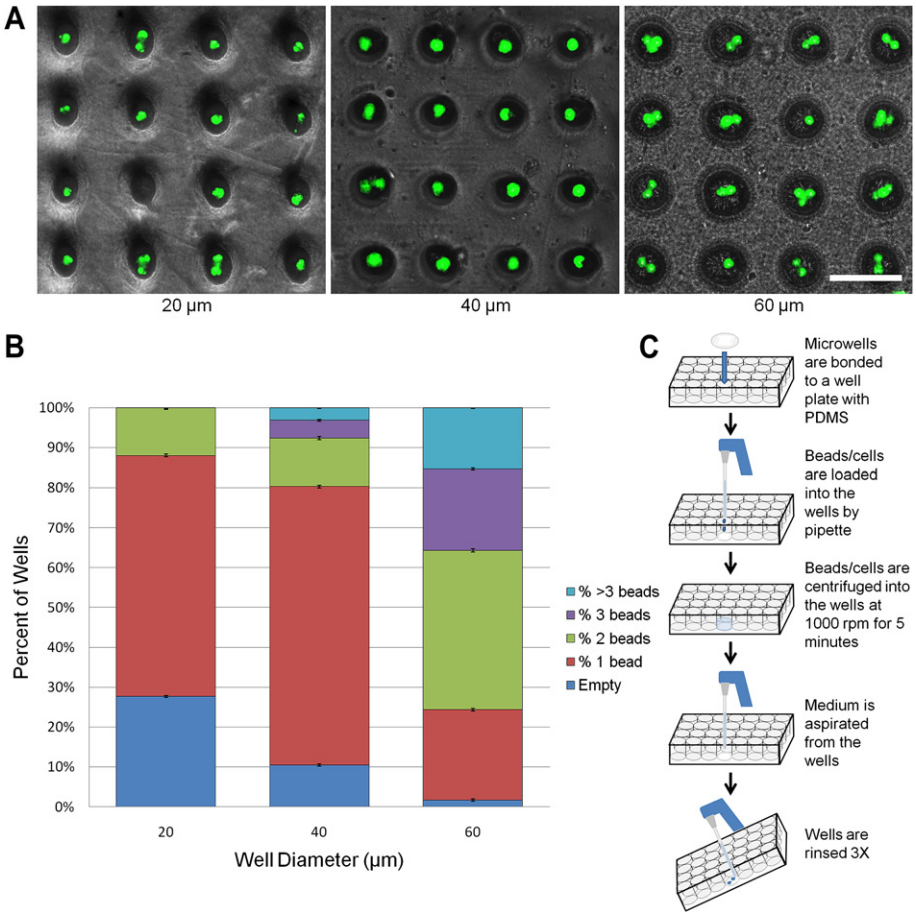

Figure 6. Bead loading. (A) 20-, 40-, and 60-µm wells loaded with 15-µm fluorescent polystyrene beads. Scale bar is 100 µm. (B) Loading efficiency of the different sized wells. 40-µm wells yielded the highest percentage of single cells per well. (C) Cell/bead loading procedure.

of each well in a 48-well plate with PDMS. Fluorescently labeled polystyrene beads (Bangs Laboratories FS07F, Fishers, IN) of 15.5-µm diameter were mixed with 1× Dulbecco's phosphate-buffered saline (DPBS) (Invitrogen, Carlsbad, CA) at a concentration of 1×10^6 beads/mL and vortexed to ensure even distribution of the beads. Each well was loaded with 1×10^6 beads and centrifuged at 1000 rpm for 10 min. After centrifugation, the well plate was tilted at an angle of 45°, and 1× DPBS was slowly aspirated from each well. With the well plate still tilted, the microwells were then rinsed three times with 1× DPBS.

For the cell loading experiment, we used mCherry-labeled myosin heavy chain human embryonic stem cell (hESC) line (Mercola, CA), courtesy of Conklin Lab, University of California, San Francisco, CA.[26] The stem cells were maintained on feeder-independent conditions, using stem cell medium comprising Knockout Dulbecco's modification of Eagle's medium (Gibco) supplemented with 20% Knockout serum replacer (Gibco), 1× Glutamax (Invitrogen, Carlsbad, CA), 1× nonessential amino acids (Invitrogen, Carlsbad, CA), and 0.1 mM β-mercaptoethanol (Calbiochem, EMD Chemicals, Darmstadt, Germany) conditioned for 24 h with mitotically inactivated mouse embryonic fibroblasts (Millipore, Billerica, MA). Before loading, the cells were rinsed with 1× DPBS. Next, to obtain single-cell suspensions, 1 mL of accutase (Millipore, Billerica, MA) was added to each well of a standard six-well tissue culture plate and incubated for 10 min. Once the cells detached, the accutase was inactivated with stem cell medium supplemented with 10 µm Y-27632 to facilitate the survival of the stem cells in single cell state. Cells were then pipetted gently to break up the aggregates and spun down at 400 rpm for approximately 3 min. Next, the cells were then resuspended in 100 µm calcein AM (BD Biosciences, Sparks, MD) diluted in 500 µL of 1× DPBS and incubated at 37 °C for 30 min. Cells were then spun down and rinsed with 1× DPBS. To load the wells, cells were then resuspended in 1× DPBS at a concentration of 1.2×10^6 cells/mL. Finally, 200 µL of the cell suspension were loaded into each well of the well plate containing the microwell arrays and allowed to plate down for 20 min before being rinsed using the previously described method.

Results and Discussion

Wells of deterministic size were created by using laser cut tape as a shadow mask for O_2 plasma etching of shrink-wrap film. After plasma treating the tape is removed, and the shrink-wrap film is heated for retraction. The heat causes

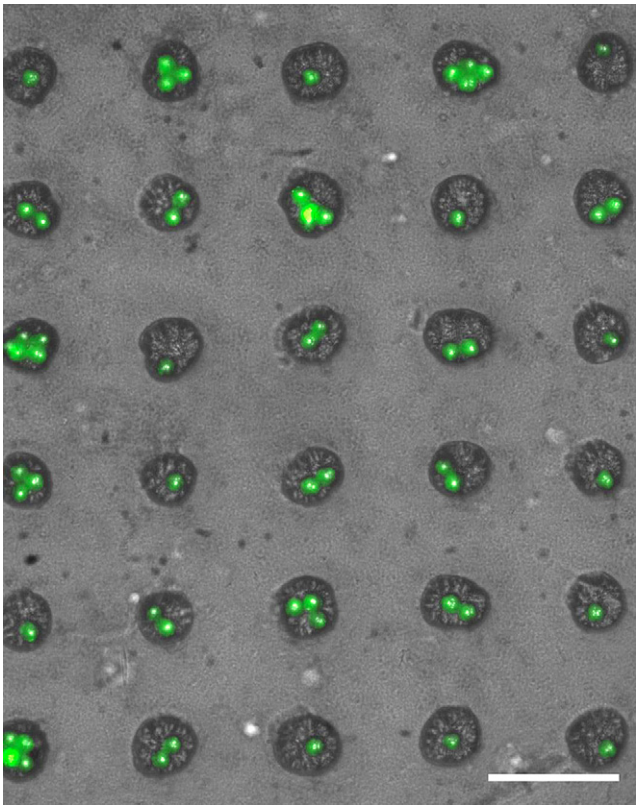

Figure 7. Loading of calcein AM-stained single human embryonic stem cells into 40-μm wells. Scale bar is 100 μm.

the polymer chains to relax and retract, resulting in high-aspect ratio wells. For example, the mask of 120 μm results in a final well size of 20 μm. Control over well size is relatively tight; the distribution of sizes for all sizes is within two standard deviations of the mean (Fig. 4). Also, the height increased linearly with plasma etch time, as expected (Fig. 5). Interestingly, the O_2 plasma etching with subsequent shrinkage results in etch shapes not achievable with traditional micromachining processes (Fig. 5B). These unique shapes, combined with the roughened surface (Fig. 2B,C), may allow for better cellular adhesion and retention in the cells after washing.

Beads were first loaded into the wells for calibration. As evidenced from Figure 6, although there is a stochastic distribution of beads in the wells, there is a large percentage of wells loaded with single cells. The roughly 70% single-cell loading efficiency of the 40-μm wells is comparable with those achievable with considerably more intensive fabrication approaches.[27] Using this platform, we successfully loaded and examined individual hESCs (Fig. 7).

Interestingly, because of the stochastic distribution of the number of cells per well, parallel studies examining the effects of single cells versus cells with one or two neighbors can thus be easily compared in the same array. Because of the large number of wells in the array, proper statistics can be achieved.

Conclusion

Here we report a novel fabrication method for the fabrication of single-cell microwell arrays of tunable sizes in commercially available commodity PO shrink films. By creating a shadow mask in tape using a CO_2 plasma, and adhering this to the thin film, exposed areas are plasma etched using an O_2 plasma. Subsequently, these etched patterns are heated to create high-aspect ratio microwells with roughened surfaces and unique mushroom-shaped geometry, which facilitates cell loading and retention during multiple washing steps. Control over well size is relatively tight; the distribution of sizes for all sizes is within two standard deviations of the mean. Notably, the process results in high-aspect ratio and high-surface-area wells. We introduce this novel fabrication method for the generation of uniform single-cell well arrays as a potential research tool for various biological applications involving longitudinal single-cell studies and cell–cell and cell–substrate interactions.

Acknowledgments

This work was supported in part by the California Institute of Regenerative Medicine, Defense Advanced Research Projects Agency N/MEMS S&T Fundamentals Program under grant no. N66001-1-4003 issued by the Space and Naval Warfare Systems Center Pacific to the Micro/Nano Fluidics Fundamentals Focus Center and Shrink Nanotechnologies, Inc.

Competing Interests Statement: Author Michelle Khine is the scientific founder of Shrink but receives no compensation nor does she have any financial interest in the company. Terms of this arrangement have been reviewed and approved by University of California, Irvine, in accordance with its conflict of interest policies.

References

1. Di Carlo, D.; Aghdam, N.; Lee, L. P. Single-cell enzyme concentrations, kinetics, and inhibition analysis using high-density hydrodynamic cell isolation arrays. *Anal. Chem.* **2006,** *78*, 4925–4930.
2. Spiller, D. G.; Wood, C. D.; Rand, D. A.; White, M. R. H. Measurement of single-cell dynamics. *Nature* **2010,** *465*, 736–745.
3. Rao, C. V.; Wolf, D. M.; Arkin, A. P. Control, exploitation and tolerance of intracellular noise. *Nature* **2002,** *420*, 231–237.
4. Ko, M. S.; Nakauchi, H.; Takahashi, N. The dose dependence of glucocorticoid-inducible gene expression results from changes in the number of transcriptionally active templates. *EMBO J.* **1990,** *9*, 2835–2842.
5. Hung, P. J.; Lee, P. J.; Sabounchi, P.; Lin, R.; Lee, L. P. Continuous perfusion microfluidic cell culture array for high-throughput cell-based assays. *Biotechnol. Bioeng.* **2005,** *89*, 1–8.
6. Bhatia, S. N.; Yarmush, M. L.; Toner, M. Controlling cell interactions by micropatterning in co-cultures: hepatocytes and 3T3 fibroblasts. *J. Biomed. Mater. Res.* **1997,** *34*, 189–199.
7. Chen, C. S.; Mrksich, M.; Huang, S.; Whitesides, G. M.; Ingber, D. E. Geometric control of cell life and death. *Science* **1997,** *276*, 1425–1428.
8. Yamamura, S.; Kishi, H.; Tokimitsu, Y.; Kondo, S.; Honda, R.; Rao, S. R.; Omori, M.; Tamiya, E.; Muraguchi, A. Single-cell microarray for analyzing cellular response. *Anal. Chem.* **2005,** 8050–8056.
9. Chang, W. C.; Lee, L. P.; Liepmann, D. Biomimetic technique for adhesion-based collection and separation of cells in a microfluidic channel. *Lab Chip* **2005,** *5*, 64–73.

10. Fu, A. Y.; Chou, H.-P.; Spence, C.; Arnold, F. H.; Quake, S. R. An integrated microfabricated cell sorter. *Anal. Chem.* **2002,** *74*, 2451−2457.
11. Carlo, D. D.; Jeong, K.-H.; Lee, L. P. Reagentless mechanical cell lysis by nanoscale barbs in microchannels for sample preparation. *Lab Chip* **2003,** *3*, 287−291.
12. Lu, H.; Schmidt, M. A.; Jensen, K. F. A microfluidic electroporation device for cell lysis. *Lab Chip* **2005,** *5*, 23−29.
13. Vilkner, T.; Janasek, D.; Manz, A. Micro total analysis systems. Recent developments. *Anal. Chem.* **2004,** *76*, 3373−3385.
14. El-Ali, J.; Sorger, P. K.; Jensen, K. F. Cells on chips. *Nature* **2006,** *442*, 403−411.
15. Lindström, S.; Eriksson, M.; Vazin, T.; Sandberg, J.; Lundeberg, J.; Frisen, J.; Andersson-Svahn, H. High-density microwell chip for culture and analysis of stem cells. *PLoS One* **2009,** *4*, e6997.
16. Moeller, H. C.; Mian, M. K.; Shrivastava, S.; Chung, B. G.; Khademhossein, A. A microwell array system for stem cell culture. *Biomaterials* **2008,** *29*, 752−763.
17. Fernandes, T. G.; Margarida Diogo, M.; Clark, D. S.; Dordick, J. S.; Cabral, J. M. S. High-throughput cellular microarray platforms: applications in drug discovery, toxicology and stem cell research. *Trends Biotechnol.* **2009,** *27(6)*.
18. Lindström, S.; Andersson-Svahn, H. Miniaturization of biological assays—overview on microwell devices for single-cell analyses. *Biochim. Biophys. Acta* **2011,** *1810*, 308−316.
19. Wood, D. K.; Weingeist, D. M.; Bhatia, S. N.; Engelward, B. P. Single cell trapping and DNA damage analysis using microwell arrays. *Proc. Natl. Acad. Sci. U.S.A.* **2010,** *107(22)*, 10008−10013.
20. Liu, C.; Liu, J.; Gao, D.; Ding, M.; Lin, J.-M. Fabrication of microwell arrays based on two-dimensional ordered polystyrene microspheres for high-throughput single-cell analysis. *Anal. Chem.* **2010,** *82*, 9418−9424.
21. Park, J. Y.; Hwang, C. M.; Lee, S. H. Ice-lithographic fabrication of concave microwells and a microfluidic network. *Biomed. Microdevices* **2009,** *11*, 129−133.
22. Young, E. W. K.; Berthier, E.; Guckenberger, D. J.; Sackmann, E.; Lamers, C.; Meyvantsson, I.; Huttenlocher, A.; Beebe, D. J. Rapid prototyping of arrayed microfluidic systems in polystyrene for cell-based assays. *Anal. Chem.* **2011,** *83*, 1408−1417.
23. Tuttle, P.; Rundell, A. E.; Webster, T. J. Influence of biologically inspired nanometer surface roughness on antigen-antibody interactions for immunoassay-biosensor applications. *Int. J. Nanomedicine* **2006,** *1(4)*, 497−505.
24. Ochsner, M.; Dusseiller, M. R.; Grandin, H. M.; Luna-Morris, S.; Textor, M.; Vogel, V.; Smith, M. L. Micro-well arrays for 3D shape control and high resolution analysis of single cells. *Lab Chip* **2007,** *7*, 1074−1077.
25. Taylor, D.; Dyer, D.; Lew, V.; Khine, M. Shrink film patterning by craft cutter: complete plastic chips with high resolution/high-aspect ratio channel. *Lab Chip* **2010,** *10*, 2472−2475.
26. Kita-Matsuo, H.; et al. Lentiviral vectors and protocols for creation of stable hESC lines for fluorescent tracking and drug resistance selection of cardiomyocytes. *PLoS One* **2009,** *4(4)*, 5046−5050.
27. Rettig, J. R.; Folch, A. Large-scale single-cell trapping and imaging using microwell arrays. *Anal. Chem.* **2005,** *77*, 5628−5634.